Development of Thermal Properties and Surface Morphology of Poly(*L*-lactic)/Chitosan Blend with Microcrystalline Cellulose Obtained from Natural Jute Fiber

Md. Sagor Hosen[1*], Md. Hafezur Rahaman[1], M. A. Gafur[2]
and Aninda Nafis Ahmed[2]

[1]*Department of Applied Chemistry and Chemical Engineering, Islamic University, Kushtia, Bangladesh.*
[2]*Pilot Plant and Process Development Center (PP & PDC), BCSIR, Dhaka, Bangladesh.*

Authors' contributions

This work was carried out in collaboration between all authors. Authors MSH and MHR designed the study, performed the statistical analysis, wrote the protocol, and wrote the first draft of the manuscript. All authors managed the analyses of the study. Authors MHR and MSH managed the literature searches. All authors read and approved the final manuscript.

Original Research Article

ABSTRACT

This research is a systematic study of how Microcrystalline cellulose (MCC) affects the thermal properties and surface morphology of Poly(*L*-lactic acid)(PLLA)/Chitosan blend by acting as reinforcement agent. MCC has high strength, high stiffness and high strain used for this work, has been obtained by acid (sulfuric acid) hydrolysis of α-cellulose extracted from jute fiber. Blends were prepared with a constant percentage (20 percent) of Chitosan and different percentage of PLLA and MCC by solution casting methods. Then samples of those blends have been characterized by Fourier-transform infrared spectroscopy (FTIR) for the confirmation of blending, Thermo-gravimetric analysis (TGA) & Differential thermal analysis (DTA) for the thermal properties measurement and

---

Corresponding author: E-mail: hosensagor@gmail.com;

Scanning electron microscope (SEM) for measuring element distribution and surface morphology. FTIR Analysis curves showed that there is no new characteristic absorption peaks appeared in the spectrum except slight shifting due to hydrogen bond and confirmed a formation of suitable blends. TGA and DTG results indicated that MCC can improve the heat resistivity of the PLLA/Chitosan blends by increasing its degradation temperature upto 5%. Comparison of DTA peaks also ensured developed thermal properties. Image of SEM shows the improvement of surface morphology.

1. INTRODUCTION

In recent years, Poly(*L*-lactide) or Poly(*L*-lactic acid) (PLLA) is approaching to the centre of polymer composites research depending upon its attractive properties and application [1-3]. Because of some excellent properties i.e. natural degradability at room temperature, non-toxicity and biocompatibility with human body, it is playing a vital role in both medical and industrial purposes [4,5]. In medical science & tissue engineering, PLLA can be used as degradable sutures, drug releasing particle and porous scaffolds for human body cell [6]. To be implanted into the tissue engineering, it should have resistivity against some bacterial or microbial infection [7]. Numerous studies have been performed for developing the antibacterial activity of PLLA by blending with other natural antibacterial agents. Among them, PLLA/Chitosan show stronger activity against the growth and activity of some bacteria. Because Chitosan has strong antibacterial activity against numbers of bacteria such as *Staphylococcus aureus and Escherichia coli* [8]. In order to develop the thermal and mechanical properties of PLLA/Chitosan di-blend, is being used with some functional additives by fabricating PLLA based composites and tri-blends [9]. In this research we investigated the effects of microcrystalline cellulose (MCC) on the thermal properties and surface morphology on PLLA/Chitosan blends. According to the previous research, natural fiber has high mechanical performance to act as a reinforcing agent in different polymeric composites [10]. MCC can form very strong particle–particle interactions between polymer matrix because of their length, flexibility, and strong hydrogen bonds, provide a better thermal resistivity [11,12]. Good dispersion with minor agglomeration provides a better surface morphology and can improve mechanical properties [13]. To the best of our knowledge, the effects of MCC on the properties of PLLA/Chitosan/MCC ternary blends have not been reported so far. The objective of this study is to develop PLLA based ternary blends with extended physical properties and also to investigate the effects of small percentages of MCC on the properties of PLLA/Chitosan/MCC blends.

2. EXPERIMENT

PLLA, used as a blend matrix, was collected from Mitsubishi Chemical Corporation, UNITIKA Plastics Division, Japan. Micro Crystalline Cellulose (MCC) was prepared from jute fiber by conventional acid hydrolysis [14]. Chitosan was derived from the partial deacetylation of chitin extracted from chemical treatment of shrimp shell [15,16]. Tossa jute (*Corchorus olitorius*) and shrimp (*Penaeus monodon*) shell was collected from southern part of Bangladesh as a raw jute and raw shell respectively.

2.1 Extraction of Chitosan from Shrimp Shell

Washed and dried raw shrimp shell was crushed to small size (approximately 0.5cm×0.5cm). Crushed shell was dipped into 1.57 M HCl solution in 1gm:10ml (w/v) ratio for 6-8 hrs at ambient temperature under constant stirring for removing mineral [17]. After washing & filtering with vacuum pump, demineralized shell, it was treated with 0.5% $KMnO_4$ in the presence of aq. $H_2C_2O_4$ for 2-3 hrs at 60-70ºC with a ratio 1g:15ml (w:v), to remove the color from the demineralized shell [18]. To separate the chitin from the protein complex it was treated with 1.25 M NaOH at 100ºC for 30 mins [19]. Deacetylation process was carried out by 50% NaOH at 100ºC for 4-5 hours at a ratio between shell & solution is 1g:20ml (w:v) to obtain pure chitosan from chitin [20].

2.2 Extraction of Micro Crystalline Cellulose from Jute Fiber

Washed raw jute fibers were dried and cut into small length (approximately 2 cm) and bleached

Table 1. Sample code and composition of different blends for the experimental purposes

Sample Code	Composition of Blend
LCMC-0	PLLA 80% + Chitosan 20%+ MCC 0%
LCMC-1	PLLA 79% + Chitosan 20%+ MCC 1%
LCMC-3	PLLA 77% + Chitosan 20%+ MCC 3%
LCMC-5	PLLA 75% + Chitosan 20%+ MCC 5%
LCMC-10	PLLA 70% + Chitosan 20%+ MCC 10%

with 0.08 M sodium chlorite ($NaClO_2$) solution along with 2M CH_3COOH, at pH 4 [21]. Bleaching was conducted at temperature 85ºC-90ºC for 90 mins with a ratio 1g:80ml (w:v). Prior to bleach, acetic acid and sodium acetate buffer solution was used to maintain constant pH. After washing and drying at 105ºC for 24 hrs, the bleached fiber was treated with 17.5% NaOH for removing of β and γ cellulose [22]. NaOH was removed from α-cellulose by washing several times with distilled H_2O and dried at 75ºC for 48 hrs using vacuum drier.

MCC was prepared from previously prepared α-cellulose by acid hydrolysis process using 64 wt% H_2SO_4. H_2SO_4 was used to break down glycoside bonds of the cellulose polymeric chain [23]. α-cellulose was treated by the acid solution for 25–30 mins at 35ºC-40ºC in a ratio 1g:10ml (w:v) with constant stirring. The reaction was immediately stopped by quenching with ice cool water to obtain gel type MCC [24]. H_2SO_4 was completely removed by washing with distilled H_2O. MCC was stored in acetone, as dispersion, by replacing H_2O by acetone with centrifugation.

2.3 Sample Preparation

Five samples of different composition were made by well-known solution casting method. Chloroform, a suitable solvent for PLLA, was used to prepare PLLA solution with continuous stirring [25]. Because of –OH group, hydrophilic property and reactivity of MCC can be increased. Therefore, it was dispersed in a non-aqueous solvent acetone with 90 mins sonication [26]. 1-2% acetic acid was used as a solvent for dissolving Chitosan [27]. To obtain the blend film, the calculated amounts of these three solutions were cast on petri dishes. Prior to cast, it was blended with vigorously stirring with a magnetic stirrer until homogenous solutions were obtained [28]. Films, obtained on petri dishes were evaporated at room temperature for 3-4 days under vacuum [29]. Sample codes were designed as LCMC-X, where L, C and MC-X mean PLLA, Chitosan and MCC with X, stand for percentages of MCC in the blend respectively (Table 1).

2.4 Sample Characterization

Shimadzu IR Prestige-21 Fourier Transform Infrared (FTIR) Spectroscopy, Japan was used to conduct FTIR analysis at a resolution of 4 cm^{-1}. KBr powder was used to make the disk by compressing with samples. For thermal properties measurement, Thermo-gravimetric analysis (TGA) and Differential thermal analysis (DTA) were conducted in a TG/DTA (SII-6300 analyzer).10 mg (approximately) of each sample was heated from 20ºC-580ºC at 15ºC min^{-1} under N_2 gas supply. Percentage of weight change and its derivative (DTG) were recorded as a function of temperature. To investigate the surface morphology and distribution of particles, Scanning electron microscope (SEM) micrograms were obtained from SEM leica AS-360FE-SEM instrument, with magnification ranging from 20X to approximately 30,000X, the spatial resolution of 50 to 100 nm.

## 3. RESULTS AND DISCUSSION

3.1 FT-IR Spectroscopy Analysis

FTIR spectroscopy technique was used to investigate intermolecular and intramoleculer interactions. The absorption peak shifting in specific regions was monitored to determine the functional group interactions due to hydrogen bonding between PLLA, chitosan and MCC. The FTIR spectrum of neat PLLA, Chitosan, MCC and LCMC-0 and LCMC-5 are depicted in Fig. 1.

In LCMC-5, a small peak was observed at 3653.18 cm^{-1} can be originated from overlapping of OH stretching N-H stretching. Broad O-H stretching band of MCC was changed to a small peak in blends [30]. Same as symmetric, Peak for O-H bond stretching (asymmetric) shifted to higher wave number from 3017.34 cm^{-1} to 3021.53 cm^{-1} indicating that bond energy increases after adding MCC. In case of C=O stretching from ester group of PLLA shifted from high region 1737.79 cm^{-1} to lower 1735.86 cm^{-1} in LCMC-0 and 1735.03 cm^{-1} in LCMC-5 confirmed that, MCC and Chitosan produce intermolecular

Table 2. Assigned peak and accounted bond for LCMC-0 & LCMC-5

| LCMC-0 Assigned Peak (cm^{-1})	LCMC-5 Assigned Peak (cm^{-1})	Accounted bond for the absorption
	3653.18	-OH stretching overlapping with N-H stretching
3017.34	3021.53	-CH stretching (Asymmetric)
2878.79	2881.68	-CH stretching (symmetric)
1735.86	1735.03	-C=O stretching
1365.65	1365.65	-CH bending
1220.96	1213.30	-C-O- stretching for Acid
1094.67	1092.73	-C-O- stretching for Alcohol

hydrogen bond between O-H and C=O group to weaken the C=O in ester group in PLLA. Similarly, other bending peaks shifted to the lower wave number caused by the intermolecular hydrogen bonding. Therefore characteristic absorption peaks were obtained from the LCMC-5, are nearly the same as LCMC-0. This can be explained based on a hypothesis that MCC is just combined with PLLA and Chitosan by hydrogen bonding interactions without forming new functional groups. Therefore, this information can provide a confirmation of a good blend formation [31].
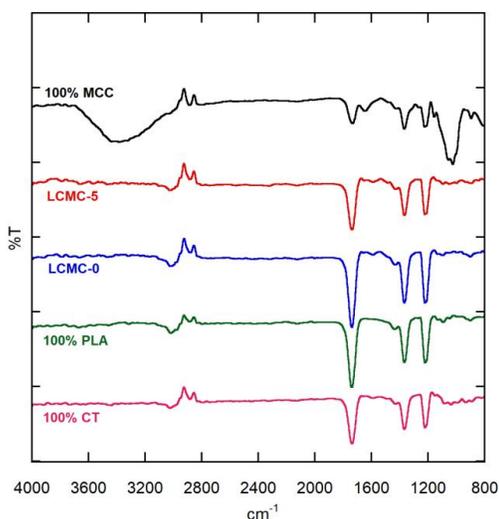
Fig. 1. Comparison of FT-IR spectra of different blends and pure components

3.2 Thermal Stability Analysis

Thermal stability was observed by Thermogravimetric analysis (TGA).

TGA data was obtained by measuring the weight loss due to degradation as a function of temperature.
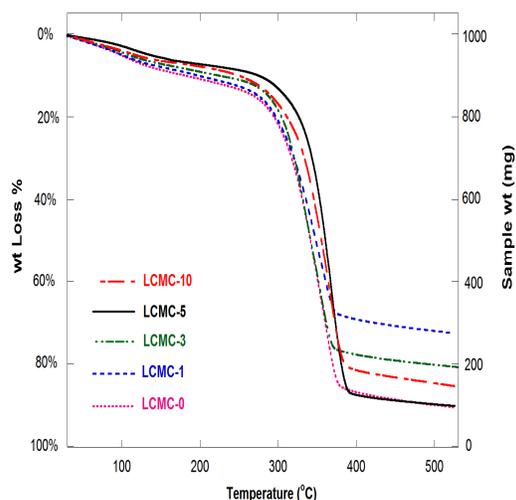
Fig. 2. Comparison between TGA curves of different blends

TGA curves have shown in Fig. 2 are the comparison of different blends with different compositions. At 80ºC to 160ºC, initial loss of moisture and desorption of gases took place, also provided information about the percentage of moisture present in the blends. Major degradation was started at approximately 300ºC and finally ended up to 390ºC. TGA analysis shows a sharp increase of initial degradation point from LCMC-0 to LCMC-5. In case of LCMC-10, each degradation point decreased with the increase of the percentage of MCC. Initial degradation point shifted from 305.3ºC to 306.8ºC, 311.3ºC and 337.2ºC for LCMC-1, LCMC-3 and LCMC-5 respectively. MCC can act as filler in the PLLA/chitosan matrix and decrease flexibility and mobility of polymeric chain by holding them tightly [32]. Therefore, the more compact composite structure can be formed with better heat resistivity. In case of LCMC-10, MCC has a tendency to accumulate by hydrogen bonding in higher percentage and

caused a sudden drop in heat degradation point to 325.5ºC [33].
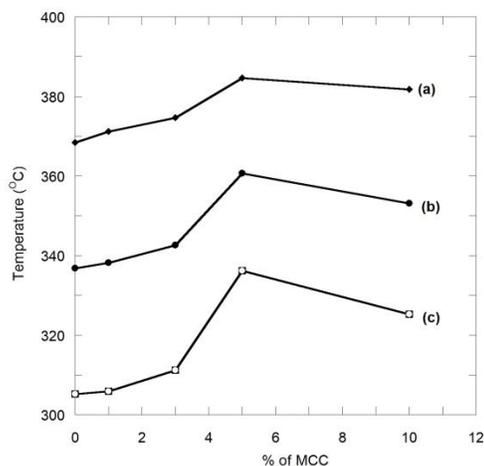

Fig. 3. Relation between % of MCC and degradation point (a) Final degradation point (b) Half degradation point (c) Initial degradation point

Half degradation point and final degradation point also showed the same pattern has given in Fig. 3. DTG data was used to determine the maximum degradation point has shown in Fig. 4. Maximum degradation point (T_{max}) increased similarly up to LCMC-5 and decreased for LCMC-10. For LCMC-0, LCMC-1, LCMC-3 and LCMC-5 the T_{max} are 357.0ºC, 358.8ºC, 362.8ºC & 374.3 respectively, and for LCMC-10 the T_{max} is placed on 371.2ºC.
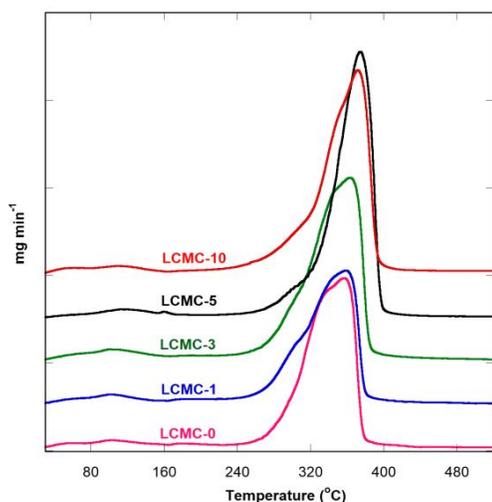

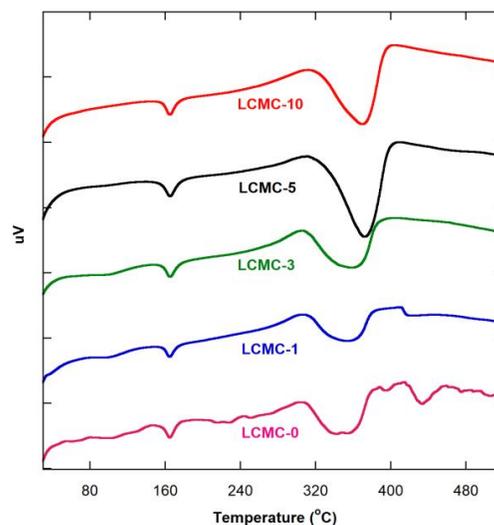**Fig. 4. Comparison between DTG curves of different blends**

Fig. 5. Comparison between DTA curves of different blends

Fig. 5 shows the change in melting point (T_m) for different blends composition depending upon the DTA curves. DTA data shows a similar trend in shifting of T_m with the addition of MCC into the blends. T_m of LCMC-0 is 162.6ºC, shifted gradually up to 165.2ºC in LCMC-5 and then similarly dropped down to 164.9ºC in LCMC-10.

T_m has been positively changed with introduction of MCC, can be described based on their intermolecular attraction between PLLA, chitosan and cellulose. Due to the formation of hydrogen bonding among PLLA, chitosan and MCC, the distance between the molecules decreases alternatively increases the molecular attraction caused high T_m [34]. However, in case of LCMC-10, low T_m may be due to the increasing of the amorphous region provided by MCC or intermolecular bond formation between consecutive cellulose units.

3.3 Surface Morphology Analysis

Fig. 6 shows the surface morphology of LCMC-0, LCMC-5 and LCMC-10 obtained from SEM microscopy. However, the surface is smoother than the other two types; relatively a large number of voids and cracks presents in the LCMC-0 caused relatively low melting point and heat degradation point. After insertion of MCC in LCMC-5, it is clearly observed that the number of pores dramatically reduced and surface looked more compact. MCC can be found inside the matrix as filler and tightly attached with the matrix caused high heat resistance capability. However

Table3. Initial, half and final degradation points of different blends

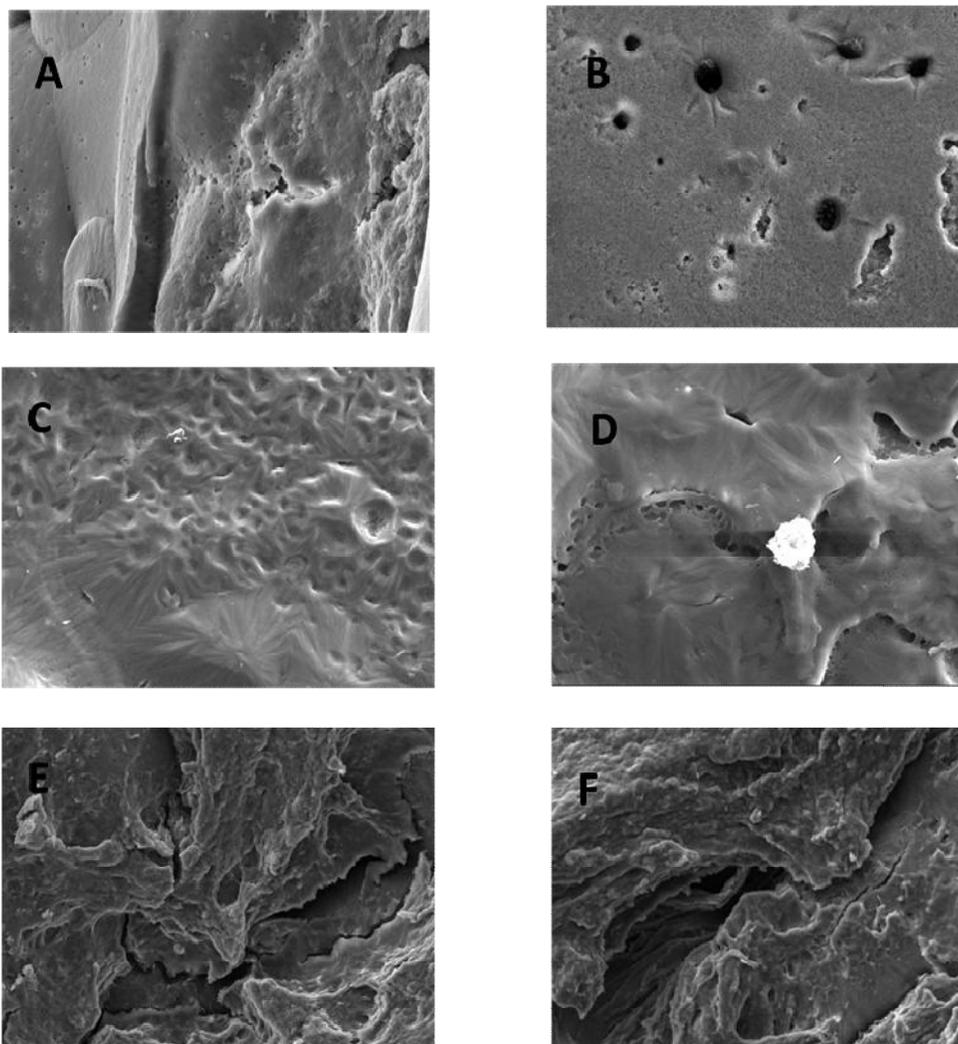| Sample name	Initial degradation point (ºC)	Half degradation point (ºC)	Final degradation point (ºC)
LCMC-0	305.3	336.8	368.4
LCMC-1	306.8	338.2	371.2
LCMC-3	311.3	342.6	374.7
LCMC-5	337.2	360.7	384.6
LCMC-10	325.5	353.1	381.8

Fig. 6. SEM micrograms for surface morphology analysis (A) LCMC-0 at 500X, (B) LCMC-0 at 1000X, (C) LCMC-5 at 500X, (D) LCMC-5 at 1000X, (E) LCMC-10 at 500X, (F) LCMC-10 at 1000X

with the increase of MCC, in LCMC-10, the surface was compacted but fractured can be ascribed as the accumulation of MCC can make that fosse structure and results the low heat degradation temperature and low melting point.

4. CONCLUSION

In this work, we studied the influence of the addition of small amounts of MCC over the thermal properties and surface morphology of

PLLA/chitosan blend. With the increase of the percentage of MCC, the thermal properties of PLLA/chitosan blends i.e. heat degradation temperature and melting point have been improved up to 5% addition of MCC in LCMC-5. In case of LCMC-10, it decreased to a lower value and concluded the maximum thermal property at LCMC-5. Surface morphology also observed and can be concluded as the surface of LCMC-5 has fewer pores and cracks than the other compositions; however, LCMC-0 showed the smoother and plain surface compared with the other.

COMPETING INTERESTS

Authors have declared that no competing interests exist.

REFERENCES

1. Yoshito I, Hideto T. Biodegradable polyesters for medical and ecological applications. Macromol Rapid Commun. 2000;21:117–132
2. Vert M, Schwarch G, Coudane J. Present and Future of PLA Polymers. J. of Macromol. Scien. Part A Pure and Applied Chemistry. 1995;32:787-796. DOI:doi.org/10.1080/10601329508010289
3. Thomson RC, Yaszemski MJ, Powers JM, Mikos AGJ. Fabrication of biodegradable polymer scaffolds to engineer trabecular bone, Journal of Biomater. Scien.: Polymer Edition. 1996;7(1):23-38
4. Hamad K, Kaseem M, Yang HW, Deri F, Ko YG. Properties and medical applications of polylactic acid: A review. eXPRESS Polymer Lett. 2015;9(5):435–455
5. Coombes AG, Meikle MC. Resorbable synthetic polymers as replacements for bone graft. Clin Mater. 1994;17(1):35-67
6. Lasprilla AJR, Martinez GAR, Lunelli BH, Jardini AL, Filho RM. Poly-lactic acid synthesis for application in biomedical devices – A review. Bio – Technology Advances. 2012;30:321–382
7. Chen X, Schluesener HJ. Nanosilver: a nanoproduct in medical application. Toxicology Letters. 2008;176(1):1–12
8. Maria C, Lı´via C, Nelson D, Lucia M. Macromolecular Symposia. 2006;245-246:515-518. DOI:10.1002/masy.200651373
9. Yan-Hua C and Ying T. Thermal and mechanical properties of poly(L-lactic acid)/ talc/1H-benzotriazole composites. Journal of Chemical and Pharmaceutical Research. 2014;6(5):734-738
10. Aji PM, Kristiina O, Mohini S. Mechanical properties of biodegradable composites from poly lactic acid (PLA) and microcrystalline cellulose (MCC). Applied Polymer Scienc. 2005;97(5):2014–2025. DOI:10.1002/app.21779
11. Rheological, mechanical, and thermal properties of polylactide/cellulose nanofiber biocomposites. Fatemeh S, Davood B, Pierre JC, Marie CH, Musa RK, Polymer composites; 2016. DOI:10.1002/pc.24127
12. Nakagaito AN, Fujimura A, Sakai T, Hama Y, Yano H. Production of microfibrillated cellulose (MFC)-reinforced polylactic acid (PLA) nanocomposites from sheets obtained by a papermaking-like process. Compos. Sci. Technol. 2009;69(7–8):1293-1297
13. Kowalczyk M, Piorkowska E, Kulpinski P, and Pracella M. Mechanical and thermal properties of PLA composites with cellulose nanofibers and standard size fibers. Compos. Part A: Appl. Sci. 2011;42:10
14. Sarwar JM, Abrar S, Zhibin H, Yonghao N. Jute as raw material for the preparation of microcrystalline cellulose. Cellulose. 2011;18(2):451–459.
15. Varshosaz J. The promise of chitosan microspheres in drug delivery systems. Expert Opinion on Drug Delivery. 2007;4:263-273
16. Tarun KV, Swaraj S, Natasha J, Jayaram C, Sohini R, Vijay BT. Extraction of chitosan and its oligomers from shrimp shell waste, their characterization and antimicrobial effect. Vet World. 2017;10(2):170–175
17. Laila M, Olfa GB, Kemel J, Islem Y, Moncef N. Extraction and Characterization of Chitin, Chitosan, and Protein Hydrolysates Prepared from Shrimp Waste by Treatment with Crude Protease from Bacillus cereus SV1. Appl. Biochem. Biotechnol. 2010;162:345–357. DOI:10.1007/s12010-009-8846-y.
18. Yuegang Z, Jian Z and Nuno C. Use of shell chitin extracted from seafood processing waste in recycling of industrial wastewater. Environmentally Conscious Manufacturing. 2001;4193. DOI:10.1117/12.417286

19. Peesan M, Supaphol P, Rujiravanit R. Preparation and characterization of hexanoyl chitosan/ polylactide blend films. Carbohydr. Polym. 2005;60:343–350.

20. Seiichi M, Masaru M, Reikichilwa M, Susumu Y. Highly deacetylated chitosan and its properties. Journal Applied Polymer Science. 1983;28:1909–1917. DOI:10.1002/app.1983.070280607

21. Morán JI, Alvarez VA, Cyras VP, Vázquez A. Extraction of cellulose and preparation of nanocellulose from sisal fibers. Cellulose. 2008;15(1):149–159

22. Cao X, Ding B, Yu J, Al-Deyab SS. Cellulose nanowhiskers extracted from TEMPO-oxidized jute fibers. Carbohydrate Polymer. 2012;90(2):1075-1080. DOI:10.1016/j.carbpol.2012.06.046

23. Vedernikov NA, Kalnina VK. Wood Cell Wall and Its Changes at Chemical Treatments. Chemistry, Riga, Latvia; 1972.

24. Thomas MG, Abraham E, Jyotishkumar P, Maria HJ, Pothen LA, Thomas S. Nanocelluloses from jute fibers and their nanocomposites with natural rubber: Preparation and characterization. International Journal of Biological Macromolecules. 2015;81:768-777

25. Madhavan NK, Nimisha RN, Rojan PJ. An overview of the recent developments in polylactide (PLA) research. Bioresource Technology. 2010;101:8493-8501

26. Mehdi J, Jalaluddin H, Aji PM, Hussein MZB, Kristiina O. Preparation of cellulose nanofibers with hydrophobic surface characteristics. Cellulose. 2010;17:299–307. DOI:10.1007/s10570-009-9387-9

27. Hong KN, Na YP, Shin HL, Samuel P. Meyer, Antibacterial activity of chitosans and chitosan oligomers with different molecular weights. International Journal of Food Microbiology. 2002;74:65-72.

28. Hideto TS, Suong HH, Yoshito I. Modification of physical properties of poly(L-lactic acid) by addition of methyl-β-cyclodextrin. Macromolecules. 1991;24(20):5651–5656. DOI:10.1021/ma00020a026

29. Hideto TS, Ikada Y. Stereocomplex formation between enantiomeric poly(lactic acid)s. XI. Mechanical properties and morphology of solution-cast films. Polymer. 1999;40:6699-6708

30. Person FG, Marchessault RH, Liang CY. Infrared spectra of crystalline polysaccharides V. Chitinp. J Polym Sci. 1960;43:101-107

31. Ping Q, Yuan G, Guo-feng W, Li-ping Z. PLA/cellulose nanocomposites. Bio Resources. 2010;5(3):1811-1823

32. Khoo RZ, Ismail H, Chow WS. Thermal and morphological properties of poly (lactic acid) / nanocellulose nanocomposites. Procedia Chemistry. 2016;19:788–794.

33. Fortunati E, Armentano I, Zhou Q, Lannoni A, Saino E, Visai L. Multifunctional bionanocomposite films of poly (lactic acid), cellulose nanocrystals and silver nanoparticles. Carbohydrate Polymers. 2012;87(2):1596-1605

34. Lin D, Dan L, Jing H. Degradation of graft polymer and blend based on cellulose and poly(L-lactide). J. APPL. POLYM. SCI. 2013;130(4):2257–2264. DOI:10.1002/app.3945